Lattice-constant dependence of the dynamical effective charge in AlAs and GaAs

G. S. Spencer, A. C. Ho, and J. Menéndez
Department of Physics, Arizona State University, Tempe, Arizona 85287-1504

R. Droopad, H. Fathollahnejad, and G. N. Maracas
Department of Electrical Engineering, Arizona State University, Tempe, Arizona 85287-5706

(Received 28 April 1994)

We have used Raman spectroscopy to study the lattice-constant dependence of the optical-phonon frequencies in AlAs and GaAs. From these studies, we deduce the dynamical effective charge for AlAs to be $e_T^*=2.20\pm0.01-(5.8\pm0.1)(-\Delta a/a_0)$. For GaAs we find a dynamical effective charge $e_T^*=2.18\pm0.01-(4.8\pm0.7)(-\Delta a/a_0)-(28\pm16)(-\Delta a/a_0)^2$. First-principles calculations, recently confirmed by experiment, indicate that the interatomic force constants (related to the second derivative of the interatomic potential) are virtually identical for GaAs and AlAs. The results reported in this paper indicate that higher-order derivatives of the interatomic potential are also remarkably similar for these two materials.

I. INTRODUCTION

GaAs, AlAs, and their alloys are the preferred system for heterostructure fabrication. Their near lattice match allows structures to be fabricated with minimal epitaxial stress. The tunability of the band gap in the alloys can be used to grow quantum-well systems with variable barrier heights. The similarity of the lattice constants in GaAs and AlAs indicate that the interatomic potentials of the two materials have their minima at about the same atomic separation. This is reflected in the calculated valence charge densities, which are almost indistinguishable.[1] Additional striking similarities between the interatomic potentials of GaAs and AlAs have been discovered in recent first-principles calculations of phonons. These studies indicate that the interatomic force constant matrices for GaAs and AlAs are very similar,[2] so that from the point of view of lattice dynamics the GaAs-AlAs heterostructure is virtually reduced to a mass perturbation problem. This result has very important practical implications, since it allows a first-principles determination of the phonon properties of disordered $Al_xGa_{1-x}As$ systems.[3] We have recently been able to confirm the remarkable similarity of the GaAs and AlAs force constants by performing second-order Raman scattering on AlAs and comparing the second-order Raman spectra with the first-principles density of states.[4] Similar results have been found in a study performed concurrently by Wagner *et al.*[5]

Since the value of the lattice constant is related to the first derivative of the potential-energy function for the lattice, and the force constants correspond to the second derivatives, it is interesting to compare the similarities of higher-order potential derivatives for GaAs and AlAs. These higher-order terms represent anharmonic effects, such as the lattice-constant dependence of the mode frequencies. In this paper, we report studies of the pressure dependence of the longitudinal-optic (LO) and transverse-optic (TO) phonon frequencies in AlAs and GaAs which indeed show the lattice-compression dependence of the effective charge, as well as the short-range contribution to the interatomic force constants, to be very similar.[6]

Since its advent several decades ago, the diamond-anvil cell has become a common tool in experimental high-pressure physics. Together with the ruby fluorescence manometer,[7] it provides an environment of known high hydrostatic pressure. Application of Raman scattering to semiconductor solids under hydrostatic pressure has been widespread.[8] Studies in which the mode Grüneisen parameter γ and Born's dynamic transverse effective charge e_T^* are obtained from the longitudinal-optic (LO) and transverse-optic (TO) phonons have been completed for many semiconductor materials. Works known to the authors are for Si and GaP;[9] GaAs;[10] ZnS, ZnSe, and ZnTe;[11] InP;[12] SiC;[13] AlN, BN, and BP;[14] and GaSb, InAs, and InSb.[15] In a recent paper, Venkateswaran *et al.* have determined the pressure dependence of the LO and TO modes in GaAs and AlAs.[16]

II. EXPERIMENT

Raman-scattering experiments were performed on AlAs grown by molecular-beam epitaxy (MBE). The sample was grown by depositing 0.5 μm of AlAs on the (001) face of a GaAs substrate. The AlAs layer was capped with a 40-Å layer of GaAs to inhibit oxidation. The experimental data for GaAs is obtained from the GaAs substrate of the AlAs sample. In this way the relative error in the pressure measurements between the two samples is minimized. A study by Cui *et al.* has shown that, for optical phonons in samples of these characteristics, the pressure dependence of the layers is indistinguishable from the bulk response.[17] Experiments were conducted at hydrostatic pressures ranging from 1 bar to 148 kbar. Pressure was applied by the use of a diamond-

0163-1829/94/50(19)/14125(6)/$06.00

anvil cell with argon as the pressure-transmitting medium. The pressure was determined from the shifts of the ruby fluorescence lines.[7] The Raman spectra were obtained in the backscattering configuration using the 514.5-nm (2.41-eV) line of an argon-ion laser. The scattered light was dispersed by a Spex double monochromator, and collected using a Spex charge-coupled device multichannel detector. All spectra were taken at room temperature.

III. RESULTS

The Raman spectra of AlAs at various pressures is shown in Fig. 1. [Note, the one-bar spectra was obtained with the sample outside of the diamond-anvil cell in the backscattering configuration off of the (001) face. In this configuration, TO-Raman scattering is forbidden. The remaining spectra were taken inside the diamond-anvil cell where the orientation of the sample is undetermined, i.e., not necessarily backscattering off of the (001) face. This accounts for the observation of TO-Raman scattering in these spectra.] As shown by the figure, as the pressure increases, the LO- and TO-phonon peaks shift to higher frequencies. This effect has been seen in other semiconductors.[9–15] A structural phase transition was observed to occur at approximately 123 kbar, in agreement with Weinstein *et al.* and Martin,[18] as well as the recent works of Venkateswaran *et al.*[16] and Greene *et al.*[19] The LO- and TO-peak positions are plotted as a function of pressure in both Figs. 1 (linearly in pressure on the right vertical scale) and 2 (nonlinearly in pressure on the top horizontal scale.) These peak positions can be accurately fit quadratically in pressure by

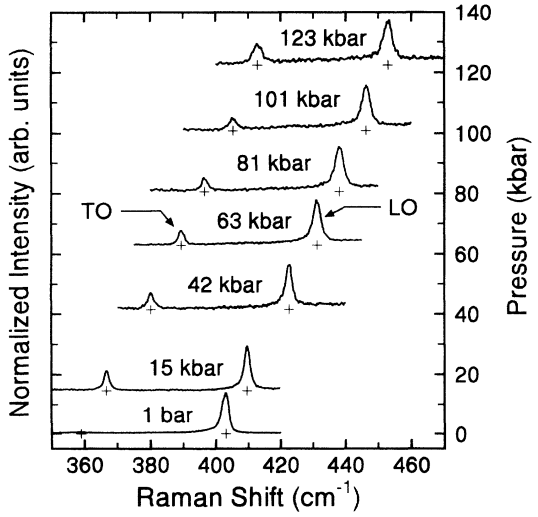

FIG. 1. The backscattering Raman spectra of AlAs is plotted for several pressures. All spectra taken at room temperature using $\lambda_L = 514.5$ nm. Optical-phonon peak positions as a function of pressure are indicated by "+." The quadratic fits of optical-phonon peak positions are given in Eq. (1).

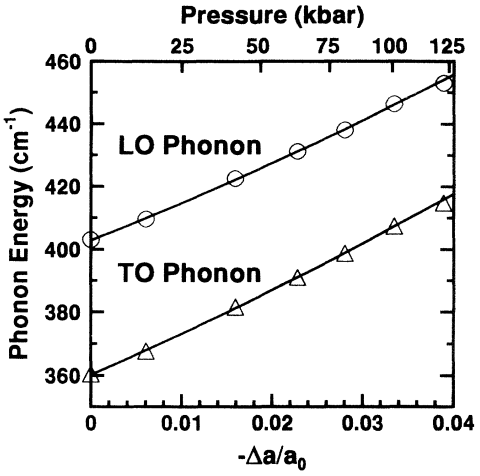

FIG. 2. LO- and TO-phonon peak positions are plotted linearly against fractional change in lattice constant and nonlinearly in pressure. The curves that passed through data are the quadratic fits in $(-\Delta a/a_0)$ of Eq. (3).

$$\begin{aligned}\omega_{\mathrm{LO}} &= 402.9\pm0.3+(0.49\pm0.02)P \\ &\quad -(0.0006\pm0.0002)P^2\ , \\ \omega_{\mathrm{TO}} &= 360.3\pm0.3+(0.53\pm0.01)P \\ &\quad -(0.0006\pm0.0001)P^2\ ,\end{aligned} \tag{1}$$

with frequency in cm^{-1} and pressure in kbar. The pressure dependence of these modes agrees well with the previous work by Venkateswaran *et al.* The fitted coefficients for the LO-phonon pressure dependence are within error of those determined by Venkateswaran *et al.*, whereas in the case of the TO-mode dependence the linear and quadratic coefficients have a somewhat different relative weight.[16] The experimental pressures are converted to lattice constant compression, $(-\Delta a/a_0)$, (a being lattice constant at pressure with the zero-pressure lattice constant $a_0 = 5.66$ Å for AlAs), using Murnaghan's equation[20]

$$P = \frac{B_0}{B_0'}\left[\left[\frac{a_0}{a}\right]^{3B_0'} - 1\right], \tag{2}$$

where B_0 is the bulk modulus and B_0' its derivative with respect to pressure. The values of B_0 and B_0' used are 770 kbar (Refs. 19 and 21) and 5 (Ref. 19), respectively. In Fig. 2 the LO- and TO-peak positions are plotted linearly against fractional lattice compression, $(-\Delta a/a_0)$, and nonlinearly against pressure. In the case of most semiconductors, ω_{LO} and ω_{TO} versus $(-\Delta a/a_0)$ fall within the experimental error of a straight line.[9,12–15] However, in the case of AlAs, the data can be fit slightly better by a quadratic fit. This is also found to be the case for GaAs.[22] The LO- and TO-peak positions fit quadratically in $(-\Delta a/a_0)$ are

$$\omega_{LO}=402.8\pm0.4+(1140\pm50)\left[-\frac{\Delta a}{a_0}\right]+(3600\pm1100)\left[-\frac{\Delta a}{a_0}\right]^2,$$
$$\omega_{TO}=360.2\pm0.4+(1230\pm40)\left[-\frac{\Delta a}{a_0}\right]+(4000\pm1100)\left[-\frac{\Delta a}{a_0}\right]^2, \quad (3)$$

in cm^{-1}. The curves of Eq. (3) are plotted with the data in Fig. 2. As can be seen from the figure, the LO-TO splitting decreases with increasing lattice compression. This decrease has been observed in most zinc-blende-type materials.[9–15] The LO-TO splitting is plotted against $(-\Delta a/a_0)$ and pressure in Fig. 3, and is fit quadratically in $(-\Delta a/a_0)$ by

$$\omega_{LO}-\omega_{TO}=42.6\pm0.1+(90\pm10)\left[-\frac{\Delta a}{a_0}\right]-(400\pm300)\left[-\frac{\Delta a}{a_0}\right]^2, \quad (4)$$

in cm^{-1}.

IV. DISCUSSION

The Grüneisen parameter, defined as $\gamma=\partial\ln\omega/\partial\ln\Omega$ where Ω is the volume of the unit cell, was found for the Γ point [$\mathbf{k}=(0,0,0)$] optic modes using the linear term of the quadratic fits in Eq. (3). The parameters obtained are $\gamma(LO_\Gamma)=0.94\pm0.05$ and $\gamma(TO_\Gamma)=1.14\pm0.04$. The LO-mode Grüneisen parameter is within error of that found by Venkateswaran *et al.*,[16] while that of the TO phonon is somewhat larger due to the difference in the fitted parameters for the TO-phonon frequencies mentioned earlier. If one wishes to predict phonon energies, it is better to generate the Grüneisen parameters from a *linear* fit of the optic frequencies in $(-\Delta a/a_0)$;

$$\omega_{LO}=402.0\pm0.5+(1280\pm20)\left[-\frac{\Delta a}{a_0}\right],$$
$$\omega_{TO}=359.4\pm0.6+(1390\pm20)\left[-\frac{\Delta a}{a_0}\right]. \quad (5)$$

The Grüneisen parameters obtained from these linear fits are $\gamma(LO_\Gamma)=1.06\pm0.02$, and $\gamma(TO_\Gamma)=1.29\pm0.02$.

In order to relate the LO-TO splitting to microscopic theory, we calculate Born's transverse effective charge e_T^*, using[23]

$$e_T^{*2}=\frac{\Omega\mu}{4\pi}\varepsilon_\infty(\omega_{LO}^2-\omega_{TO}^2), \quad (6)$$

in atomic units. Here Ω is the volume of the unit cell, μ is the reduced mass ($1/\mu=1/M_{Al}+1/M_{As}$), and ε_∞ is the infrared dielectric constant. The room pressure value of ε_∞ is taken to be 8.16.[24] Since there is no experimental data available for the volume dependence of ε_∞ for AlAs, we assume the GaAs (Ref. 25) dependence of $d\ln\epsilon_\infty/d\ln a\simeq3$ following the justification of Ref. 12. The resultant e_T^* as a function of $(-\Delta a/a_0)$ is shown in Fig. 4. As can be seen from the figure, e_T^* decreases with increasing lattice compression. This effect is similar to that for other III-V and II-VI compounds.[9–12,15] (For a discussion of the dependence of e_T^* on lattice compression, see Ref. 14.) The dependence of e_T^* on $(-\Delta a/a_0)$ is fit very well by the linear function

$$e_T^*(AlAs)=2.20\pm0.01-(5.8\pm0.1)\left[-\frac{\Delta a}{a_0}\right], \quad (7)$$

in cm^{-1}. This function is plotted as the solid line in Fig. 4.

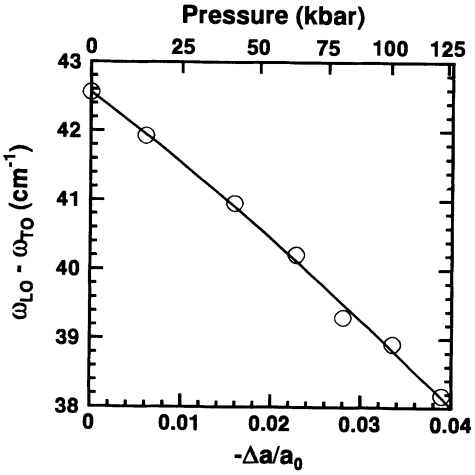

FIG. 3. The splitting of LO- and TO-phonon modes is plotted linearly against fractional change in lattice constant and nonlinearly against pressure. The curve that passed through points is the quadratic fit in $(-\Delta a/a_0)$ of Eq. (4).

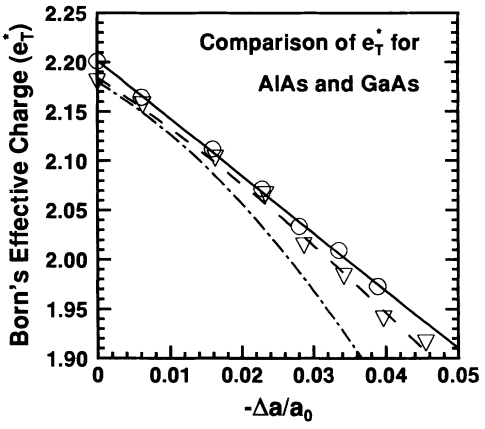

FIG. 4. The experimental lattice-compression dependence of Born's transverse effective charge for AlAs (GaAs) is plotted as circles (triangles). The linear and quadratic fits of Eqs. (7) and (8) are plotted as the solid and dotted lines, respectively. Also plotted is the quadratic fit of Trommer *et al.* for GaAs [Eq. (9)] (Ref. 12).

For GaAs, we calculate the lattice compression [Eq. (2)] and the transverse effective charge [Eq. (6)] using the parameters $B_0=750$ kbar,[21] $B_0'=4.67$,[26] $d\ln\epsilon_\infty/d\ln a \simeq 3$,[25] and room pressure $\epsilon_\infty=10.9$.[27] The mode Grüneisen parameters obtained from the linear fits to the phonon frequency dependence on lattice compression are $\gamma(\mathrm{LO}_\Gamma)=1.15\pm0.02$, and $\gamma(\mathrm{TO}_\Gamma)=1.34\pm0.03$. These values are in reasonably good agreement with previous results.[28] The calculated experimental e_T^* are represented by triangles in Fig. 4. These points are best fit by the quadratic function

$$e_T^*(\mathrm{GaAs})=2.18\pm0.01-(4.8\pm0.7)\left[-\frac{\Delta a}{a_0}\right]-(28\pm16)\left[\frac{-\Delta a}{a_0}\right]^2, \quad (8)$$

in atomic units. This function is plotted as the dashed line in Fig. 4. Also plotted in Fig. 4 as the dot-dashed line is the quadratic fit for GaAs of Trommer *et al.*,[12]

$$e_T^*(\mathrm{GaAs})=2.18-4.4\left[-\frac{\Delta a}{a_0}\right]-88\left[-\frac{\Delta a}{a_0}\right]^2, \quad (9)$$

in atomic units. Note that although these two fits differ somewhat, the zero-pressure values and the direction of curvature are the same.

Upon inspection of Fig. 4, several observations can be made. First, the zero-pressure values for the transverse effective charge of GaAs and AlAs are separated by less than 1%. (The values of the transverse effective charge for III-V and II-VI semiconductors tabulated in Ref. 25 have a standard deviation of 0.33 or 14%.) Second, although the dependence for AlAs is more linear than that of GaAs, the difference between their transverse effective charges remains small for all values of the lattice constant. (Slopes of the linear fit for the dependence of the effective charge on lattice compression range from approximately -1 to -10 for III-V materials.)

The similarity of the long-range interaction (effective charge) together with that of the mode Grüneisen parameters implies that the short-range components of the interatomic potential for GaAs and AlAs should also be similar. An explicit comparison of the short-range terms is made in Fig. 5. We calculate the short-range contribution $\mu\omega_{\mathrm{SR}}^2$ to the interatomic force constants using[29]

$$\mu\omega_{\mathrm{SR}}^2=\omega_{\mathrm{LO}}^2-\tfrac{2}{3}(\omega_{\mathrm{LO}}^2-\omega_{\mathrm{TO}}^2), \quad (10)$$

where, again, μ is the reduced mass. Clearly, AlAs and GaAs have a very similar lattice-compression dependence of the short-range force constants that determine the optical-phonon frequencies.

To establish the link between the experimental transverse effective charge of AlAs and theory, we use two classic models for the dependence of e_T^* on lattice compression. The first is a semiempirical model of the tetrahedral bond: the bond-orbital model (BOM).[30] In this model Born's transverse effective charge is given by

$$e_T^*=-\Delta Z+\tfrac{20}{3}\alpha_p-\tfrac{8}{3}\alpha_p^3, \quad (11)$$

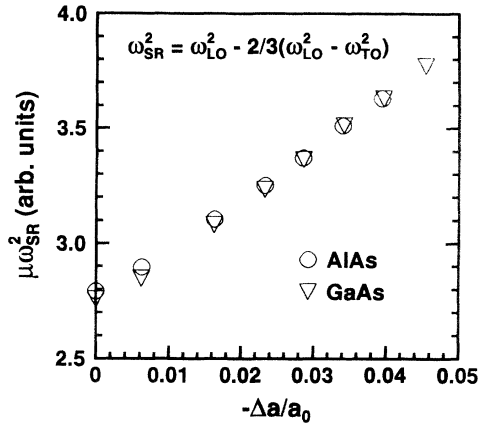

FIG. 5. The lattice-compression dependence of the short-range contribution to the interatomic force constants for AlAs (circles) and GaAs (inverted triangles) is plotted. Note the strong similarity for these compounds.

where ΔZ is one-half the difference in core charge between the anion and cation ($\Delta Z=1$ in atomic units for all III-V materials), and α_p is the polarity or ionicity parameter for the bond defined by Harrison and Ciraci.[31] The parameter α_p can be expressed[30]

$$\alpha_p=\frac{V_3}{\sqrt{V_2^2+V_3^2}}. \quad (12)$$

Here V_2 is the sp^3 hybrid covalent energy gap and V_3 is the polar energy.[30] In the BOM, the dependence of V_2 on

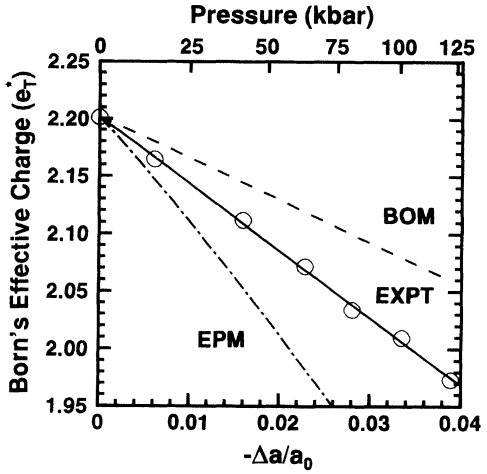

FIG. 6. Born's transverse effective charge, calculated using Eq. (6), is plotted linearly against fractional change in lattice constant and nonlinearly against pressure. The line that passed through points is the linear fit in $(-\Delta a/a_0)$ of Eq. (7). The theoretical transverse effective charge calculated by the bond-orbital model and the empirical pseudopotential model are indicated by the dashed and dot-dashed lines, respectively. Both theoretical calculations have been multiplied by a factor in order to give the experimental zero-pressure values of Born's transverse effective charge.

$(-\Delta a/a_0)$ is taken to be proportional to a^{-2}, while V_3 is taken to be independent of a. The zero-pressure values of the gap parameters for AlAs used are $V_2^0=2.79$ eV and $V_3^0=1.53$ eV.[30] In Fig. 6, the AlAs transverse effective charge experimental data (circles) and linear fit (solid line) are plotted along with the result of the BOM calculation (dashed line).

The second model we use to calculate the dependence of e_T^* on $(-\Delta a/a_0)$ is the empirical pseudopotential model (EPM).[12,15,32,33] We follow the method outlined in Refs. 12 and 15, where only the pseudopotential form factors for two reciprocal-lattice vectors are used in the calculation of e_T^*. The two reciprocal-lattice vectors are G(111) and G(220), and their pseudopotential form factors are represented by $v_\alpha(3)$ and $v_\alpha(8)$, respectively ($\alpha=1$ for cation, $\alpha=2$ for anion). In this simplified version of the EPM the transverse effective charge is given by

$$e_T^*=-\Delta Z-4\frac{v_A(8)+2v_S(3)v_A(3)/E_x}{v_S(8)+\{v_S^2(3)+v_A^2(3)\}/E_x}\ , \tag{13}$$

where, again, ΔZ is one-half the difference in core charges and

$$v_S=\tfrac{1}{2}(v_1+v_2)\ ,$$
$$v_A=\tfrac{1}{2}(v_1-v_2)\ , \tag{14}$$
$$E_x=\tfrac{1}{2}\left[\frac{2\pi}{a}\right]^2\ .$$

For zero pressure, we take the atomic pseudopotential form factors of Andreoni and Car, which are fit to empirical results.[34] The lattice-constant dependence for the transverse charge was obtained using the model pseudopotential

$$v(\mathbf{G})=\frac{8\pi Z}{G^2\varepsilon_G}\frac{\cos(\mathbf{G}\cdot\mathbf{R}_c)}{\Omega}\ . \tag{15}$$

Here $G=2\pi/a$, ε_G is the dielectric function, Ω is the volume of the unit cell, and R_c is the core radius. The values for the core radius taken for this calculation are $R_c(\mathrm{Al})=1.15$ a.u. and $R_c(\mathrm{As})=0.96$ a.u.[30] The dielectric function is slowly varying in G. Therefore, its contribution to the lattice-compression dependence is neglected. The pressure dependence of the transverse effective charge thus calculated is shown in Fig. 6 by the dot-dashed line.

In Fig. 6 the dependence of e_T^* on lattice compression calculated using the EPM (BOM) is shown to be larger (smaller) than that observed experimentally. This effect is found for most III-V compounds.[9,12,15] (Exceptions are the larger band-gap materials BN, BP, and AlN. See Ref. 14.)

V. CONCLUSIONS

We have measured the lattice-compression dependence of Born's transverse effective charge and the short-range contribution to the interatomic potential for GaAs and AlAs. The lattice-constant dependence of these properties are seen to have strong similarities for these materials. This demonstrates that the similarity of GaAs and AlAs can be seen in not only the first (lattice constants) and second (force constants) derivatives of the potential-energy function, but also in higher-order derivatives.

ACKNOWLEDGMENTS

We wish to acknowledge the assistance of Roland Hanson in this work. This study has been supported by the National Science Foundation under Grant Nos. DMR-88-14918 and DMR 91-21567.

[1]N. E. Christensen, S. Satpathy, and Z. Pawlowski, Phys. Rev. B **36**, 1032 (1987).
[2]P. Giannozzi, S. Gironcoli, P. Pavone, and S. Baroni, Phys. Rev. B **43**, 7238 (1991).
[3]E. Molinari, S. Baroni, P. Giannozzi, and S. de Gironcoli, Phys. Rev. B **45**, 4280 (1992).
[4]G. S. Spencer, J. Grant, R. Gray, J. Zolman, J. Menéndez, R. Droopad, and G. N. Maracas, Phys. Rev. B **49**, 5761 (1994).
[5]J. Wagner, A. Fischer, W. Braun, and K. Ploog, Phys. Rev. B **49**, 7295 (1994).
[6]For a review of morphic effects in lattice dynamics, see E. M. Anastassakis, in *Dynamical Properties of Solids,* edited by G. K. Horton and A. A. Maradudin (North-Holland, New York, 1980), Vol. 4, p. 157.
[7]J. D. Barnett, S. Block, and G. J. Piermarini, Rev. Sci. Instrum. **44**, 1 (1973); G. J. Piermarini, S. Block, J. D. Barnett, and R. A. Forman, J. Appl. Phys. **46**, 2774 (1975).
[8]For a review see B. A. Weinstein and R. Zallen, in *Light Scattering in Solids IV,* edited by M. Cardona and G. Güntherodt (Springer-Verlag, Berlin, 1984), Chap. 8.
[9]B. A. Weinstein and G. J. Piermarini, Phys. Rev. B **12**, 1172 (1975).
[10]R. Trommer, E. Anastassakis, and M. Cardona, in *Light Scattering in Solids,* edited by M. Balkanski, R. C. C. Leite, and S. P. S. Porto (Flammarion, Paris, 1976), p. 396.
[11]B. A. Weinstein, Solid State Commun. **24**, 595 (1977).
[12]R. Trommer, H. Müller, M. Cardona, and P. Vogl, Phys. Rev. B **21**, 4869 (1980).
[13]D. Olego, M. Cardona, and P. Vogl, Phys. Rev. B **25**, 3878 (1982).
[14]J. A. Sanjurjo, E. López-Cruz, P. Vogl, and M. Cardona, Phys. Rev. B **28**, 4579 (1983).
[15]K. Aoki, E. Anastassakis, and M. Cardona, Phys. Rev. B **30**, 681 (1984).
[16]U. D. Venkateswaran, L. J. Cui, B. A. Weinstein, and F. A. Chambers, Phys. Rev. B **45**, 9237 (1992).
[17]L. J. Cui, U. D. Venkateswaran, B. A. Weinstein, and F. A. Chambers, Semicond. Sci. Technol. **6**, 469 (1991).
[18]B. A. Weinstein, S. K. Hark, R. D. Burnham, and R. M. Martin, Phys. Rev. Lett. **58**, 781 (1987); B. A. Weinstein, S. K. Hark, and R. D. Burnham, in *Proceedings of the Eighteenth International Conference on the Physics of Semiconductors,* edited by O. Engström (World Scientific, Singapore, 1986), p. 707; R. M. Martin, *ibid.*, p. 639.

[19]R. G. Greene, H. Luo, T. Li, and A. L. Ruoff, Phys. Rev. Lett. **72**, 2045 (1994).
[20]F. D. Murnaghan, Proc. Natl. Acad. Sci. U.S.A. **30**, 244 (1944).
[21]M. L. Cohen, Phys. Rev. B **32**, 7988 (1985).
[22]R. Trommer, Ph.D. thesis, University of Stuttgart, 1977; GaAs quadratic fits reproduced in Ref. 5.
[23]M. Born and K. Huang, *Dynamical Theory of Crystal Lattices* (Clarendon, Oxford, 1954), Chap. 2.
[24]R. E. Fern and A. Onton, J. Appl. Phys. **42**, 3499 (1971).
[25]W. A. Harrison, Phys. Rev. B **14**, 702 (1976).
[26]H. J. McSkimin, A. Jayaraman, and P. Andreatch, J. Appl. Phys. **38**, 2362 (1967).
[27]C. J. Johnson, G. H. Sherman, and R. Weil, Appl. Opt. **8**, 1667 (1969).
[28]R. Trommer, Ph.D. thesis, University of Stuttgart, 1977.
[29]P. Brüesch, in *Phonons: Theory and Experiments I* (Springer-Verlag, Berlin, 1982), Chap. 4.
[30]W. Harrison, *Electronic Structure and Properties of Solids* (Freeman, San Francisco, 1980).
[31]W. A. Harrison and S. Ciraci, Phys. Rev. B **10**, 1516 (1974).
[32]M. L. Cohen and V. Heine, in *Solid State Physics,* edited by H. Ehrenreich, F. Seitz, and D. Turnbull (Academic, New York, 1970), Vol. 24, p. 37.
[33]P. Vogl, J. Phys. C **11**, 251 (1978).
[34]W. Andreoni and R. Car, Phys. Rev. B **21**, 3334 (1980).